Received: 15 December 2022 | Revised: 7 January 2023 | Accepted: 9 January 2023

DOI: 10.1002/pol.20220745

RESEARCH ARTICLE

JOURNAL OF POLYMER SCIENCE WILEY

Assembly–disassembly switching of chiral sheet assembly for controlled circularly polarized luminescence

Longlong Dong[1] | **Dawoon Lee**[2] | **Yongju Kim**[2,3] | **Myongsoo Lee**[1]

[1]Department of Chemistry, Fudan University, Shanghai, China

[2]KU-KIST Graduate School of Converging Science and Technology, Korea University, Seoul, Republic of Korea

[3]Department of Integrative Energy Engineering, Korea University, Seoul, Republic of Korea

Correspondence
Yongju Kim, KU-KIST Graduate School of Converging Science and Technology, Department of Integrative Energy Engineering, Korea University, Seoul 02841, Republic of Korea.
Email: youngjukim@korea.ac.kr

Myongsoo Lee, Department of Chemistry, Fudan University, Shanghai 200438, China.
Email: mslee@fudan.edu.cn

Funding information
National Natural Science Foundation of China, Grant/Award Numbers: 21971084, 92156023, 22150710515; National Research Foundation of Korea, Grant/Award Numbers: NRF-2022R1F1A1075138, NRF-2022R1A4A1031687

Abstract

Although substantial advances have been made regarding synthetic chiral assemblies, obtaining the two-dimensional (2D) system with a sophisticated supramolecular chirality remains challenging. Herein, we report the switchable supramolecular chiral 2D materials via donor-acceptor interaction between a pyrene amphiphile and 7,7,8,8-tetracyanoquinodimethane (TCNQ). The resulting supramolecular chiral sheets spontaneously disassemble when TCNQ is irreversibly photo-reduced to its anion. Subsequent additions of TCNQ drive the disassembled molecules to repeatedly form optically active sheet structures, demonstrating that the assembled materials exist transiently only while TCNQ is supplied. The chiral sheets emit intense circularly polarized light with a large luminescence dissymmetric factor (g_{lum}).

KEYWORDS

charge–transfer interaction, chiral sheets, circularly polarized luminescence, self-assembly, switchable supramolecules

1 | INTRODUCTION

Supramolecular systems provide sophisticated nanomaterials that exhibit diverse structures and functions.[1,2] For example, synthetic aromatic amphiphiles can self-assemble into tubules, fibers, porous sheets, and vesicles.[3,4] Interestingly, the resulting self-assembled materials become switchable when triggered by external stimuli such as guest molecules, pH, solvent, and temperature.[5] In terms of the design of supramolecular switchable systems, the introduction of chirality is a key issue because supramolecular chirality brings about unique material properties.[6,7] The coupling between the chiral and chromatic molecules through non-covalent bonds is a general strategy for the formation of chiral supramolecular materials.[8] The interactions between light and chiral species result in unique chiroptical signals described as optical rotatory dispersion (ORD), circular dichroism (CD), and circularly polarized luminescence (CPL).[9–11] Supramolecular chiral switchable systems have recently attracted great attention. For example, Adam et al. introduced the light-switchable CPL process through the three isomeric states of azobenzene moiety step by step (*trans* → *cis*-(*M*) → *cis*-(*P*)).[12] Miao et al. used the enantiomeric glutamate gelators containing a spiropyran moiety to develop reversibly transformable mirror-imaged nanohelical fibers for CPL.[13] Although extensive studies have been conducted on switchable chiroptical supramolecular materials with different dimensions, little has been reported on well-defined-two-dimensional (2D) chiroptical materials by

By Invitation Only: Tribute Special Issue dedicated to Prof. Takuzo Aida.

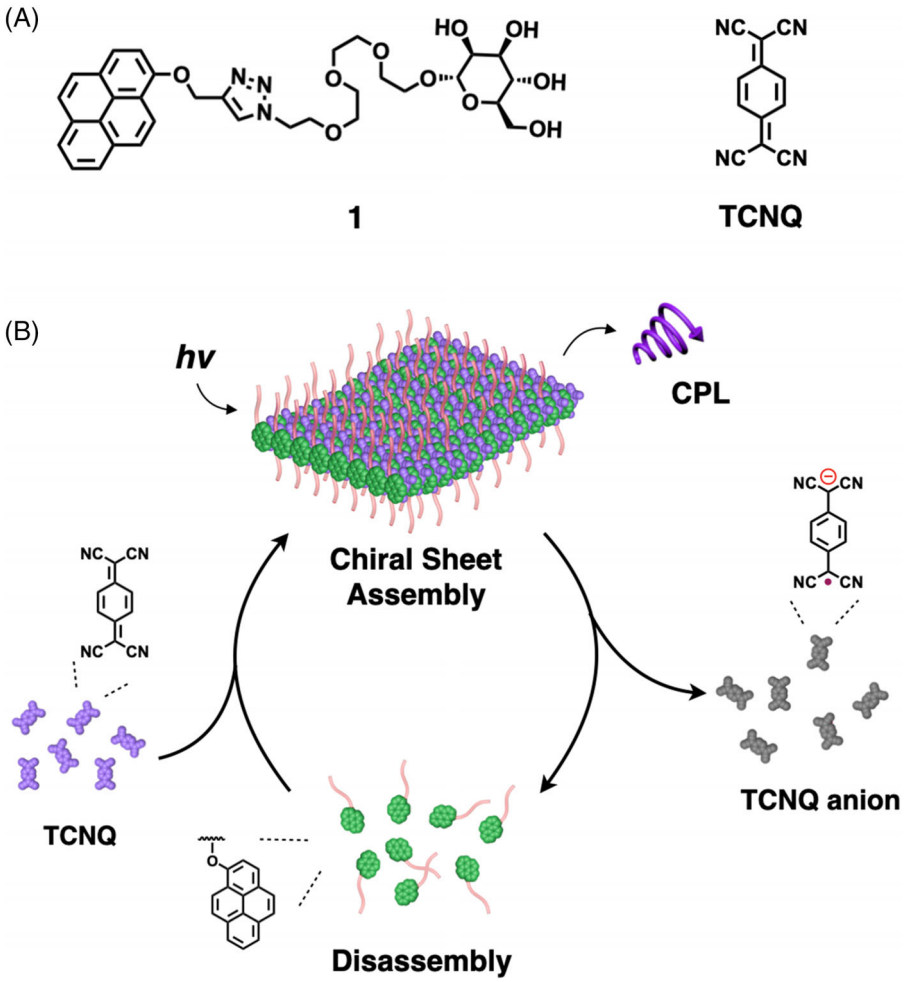

FIGURE 1 Switchable supramolecular chiral sheets triggered by TCNQ. (A) Molecular structures of amphiphile **1** and TCNQ. (B) Schematic representation of a TCNQ-driven switchable chiral sheet showing CPL.

supramolecular approach. 2D chiroptical materials can provide a novel perspective in the development of functional materials due to the physical and chemical properties of 2D structures, attributed to their large surface area and flexibility.[14,15]

Here, we report a switchable supramolecular chiral 2D structure via donor-acceptor interactions between π-electron rich pyrene and π-electron deficient 7,7,8,8-tetracyanoquinodimethane (TCNQ) in an aqueous solution (Figure 1). In the presence of TCNQ as an acceptor, amphiphile **1** (donor) self-assembles into sheet structures that exhibit an induced CD signal, indicative of the formation of supramolecular chiral sheets. Interestingly, the supramolecular chiral sheets were spontaneously disassembled upon the irreversible photoreduction of TCNQ to its anion in the aqueous solution, where the donor-acceptor interactions had collapsed. Subsequent addition of TCNQ could activate the assembly repeatedly to reform the chiral sheets, leading to a switchable supramolecular chiral system with chiroptic functionality (Figure 1). The resulting chiral sheets, driven by TCNQ, exhibited intense CPL signals with a large luminescence dissymmetric factor (g_{lum}) value of 0.046.

2 | RESULTS AND DISCUSSION

2.1 | Formation of chiral sheets by donor–acceptor interactions with TCNQ

Amphiphile **1** was composed of a hydrophobic pyrene segment and a hydrophilic D-mannose segment, where the two segments were connected by an oligoethylene glycol linker via click reaction (Scheme S1). Synthetic amphiphile **1** was characterized via nuclear magnetic resonance (NMR) spectroscopy and MALDI-TOF mass spectrometry to verify the structure presented herein (Figures S1–S3). To investigate the aggregation behavior of amphiphile **1** in an aqueous solution, negatively stained transmission electron microscopy (TEM) experiments were performed, and the micelle structures with a size of 20 nm were observed (Figure S4). A weak excimer emission of pyrene moieties was observed at approximately 500 nm in the fluorescence spectrum, indicating that the pyrene groups of **1** were mainly not in sufficient spatial proximity to form pyrene dimers for further aggregation (Figure 2B). CD signals could not be detected even through amphiphile **1** contains a chiral D-mannose side

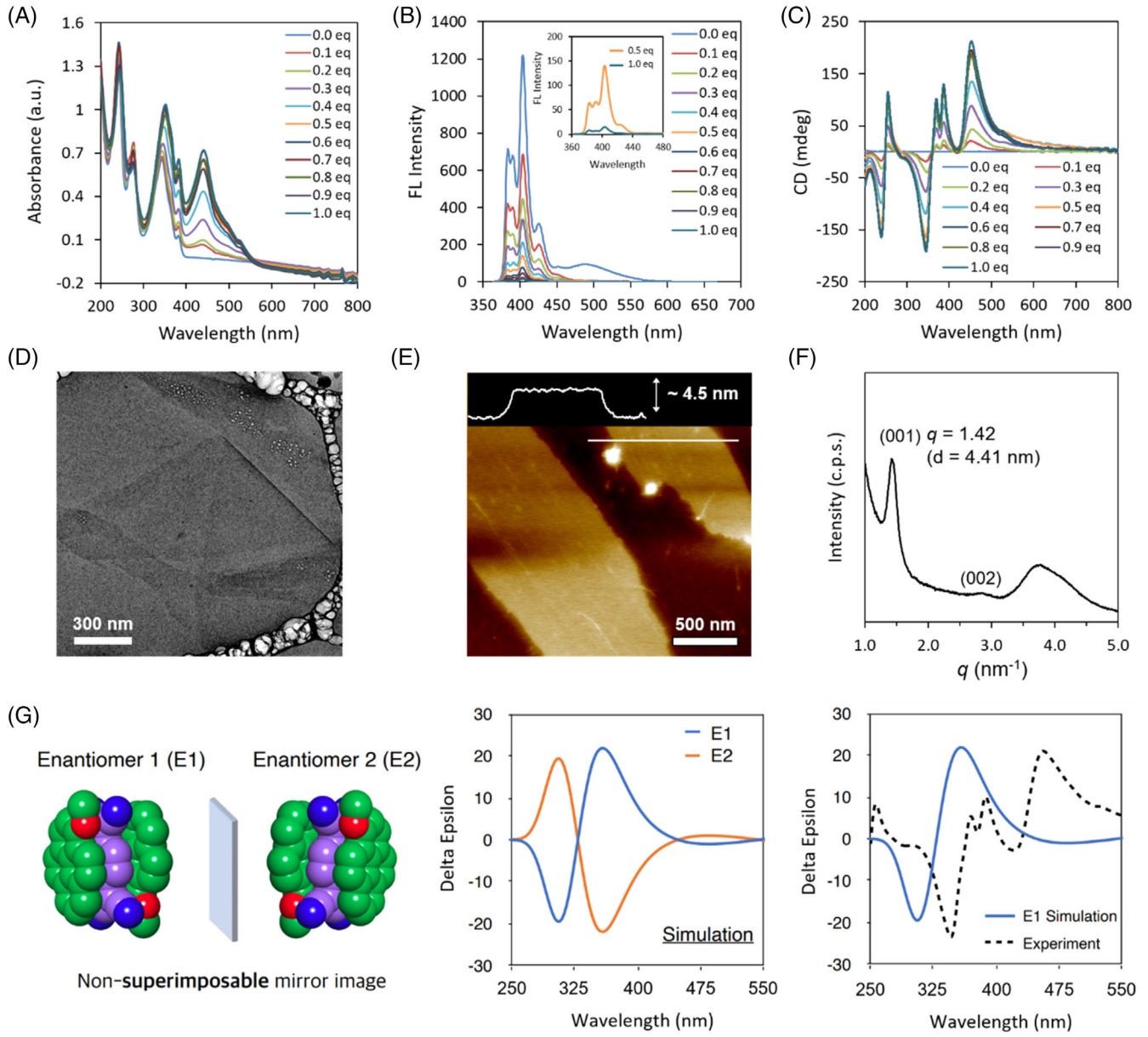

FIGURE 2 Formation of the supramolecular chiral sheets. (A) Absorption spectra, (B) emission spectra (excitation wavelength = 343 nm), and (C) CD spectra of amphiphile **1** (314 μM) with different equivalents of TCNQ in an aqueous solution. The inset of (b) shows fluorescence intensity with 0.5 equivalents and 1.0 equivalent of TCNQ. (D) Cryo-TEM image of **1** (314 μM) with 0.5 equivalents of TCNQ. (E) AFM height image of the film on a mica surface by the evaporation of **1**(314 μM) with 0.5 equivalents of TCNQ in an aqueous solution. (F) SAXS pattern of **1** with 0.5 equivalents of TCNQ after freeze-drying. (G) Representative chiral packing of CT complex and predicted CD spectra of the asymmetric packing (E1 and E2) obtained via DFT calculations.

chain, suggesting that the molecules in the aqueous solution are predominantly randomly interacting on the pyrene segments (Figure 2C).

Pyrenes are well-known to form charge-transfer (CT) complexes with π-electron deficient 7,7,8,8-TCNQ via electron donor-acceptor interactions.[16,17] Such an interaction would force pyrene units and TCNQ molecules to pack in a substantially dense and parallel arrangement. Therefore, we investigated the aggregation behavior of amphiphile **1** in the presence of TCNQ in an aqueous solution. Upon the addition of TCNQ, a characteristic broad absorption band, arising from intermolecular CT interactions was detected at approximately 441 nm (Figures 2A and S5).[18] A color change of the solution from colorless to yellow was likewise indicative of CT complexes due to the transfer of electronic charge from the donor to the acceptor (Figure S5).[16] The fluorescence of the pyrene segment had also decreased, indicating that TCNQ had formed a complex with the pyrene donor through CT interactions (Figure 2B and S6). The

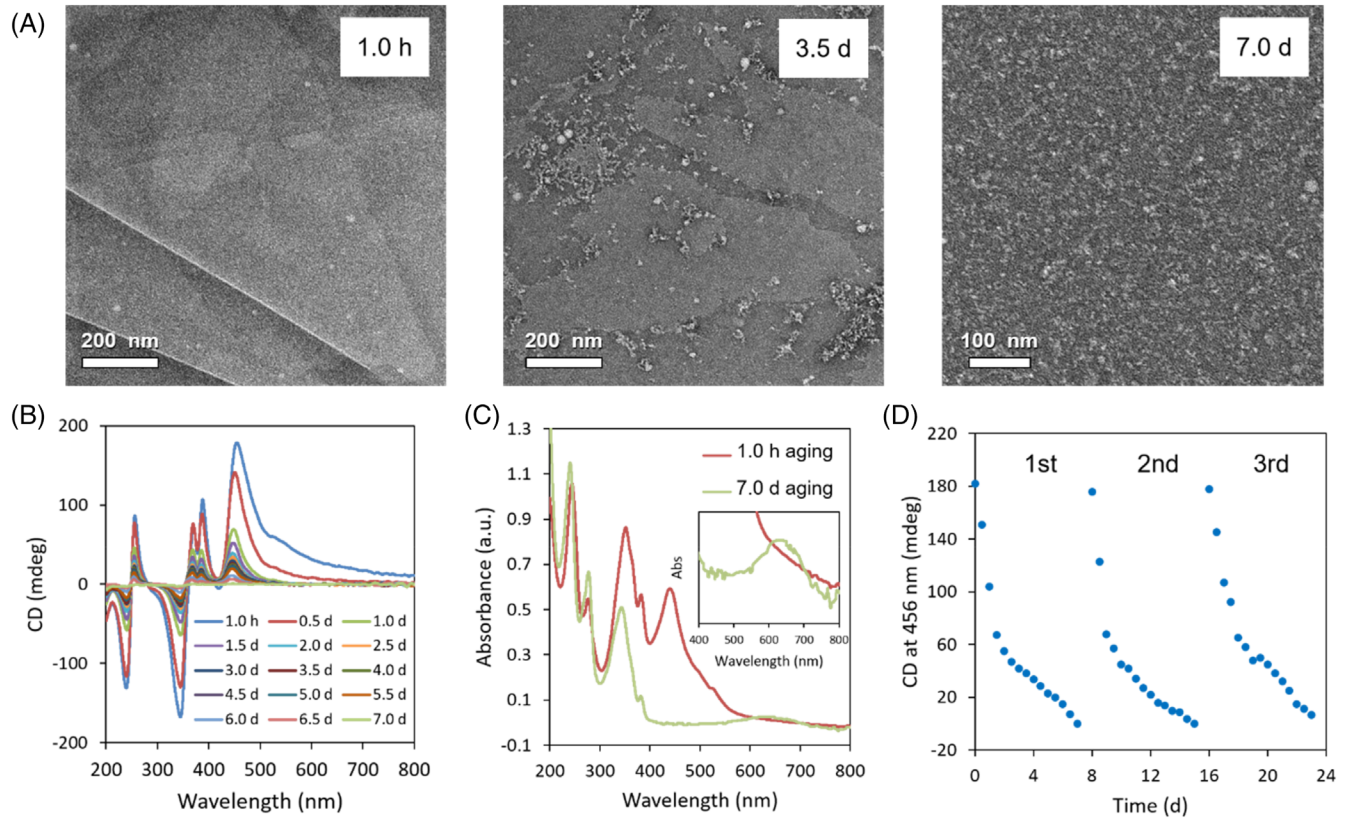

FIGURE 3 Disassembly of supramolecular chiral sheets driven by TCNQ reduction. (A) Time-dependent negatively stained TEM images, and (B) CD spectra of **1** (314 μM) with 0.5 equivalents of TCNQ in an aqueous solution. (C) Absorption spectra of **1** (314 μM) with 0.5 equivalents of TCNQ in an aqueous solution by 1.0 h (red line) aging and 7.0 d (green line) aging. (D) Repeated cycles of CD intensity, at 456 nm, of **1** (314 μM) with 0.5 equivalents of TCNQ as a function of time in an aqueous solution.

phase-contrast optical microscopy and fluorescence microscopy images showed that although a CT complex had formed, its emission with 0.5 equivalents of TCNQ was not fully quenched in contrast to the emission of the complex with 1.0 equivalents of TCNQ (Figures 2B and S7). Therefore, in order to provide an emissive CT material, 0.5 equivalents of TCNQ to **1** were chosen as the optimal stoichiometric ratio for further experiments.

TEM experiments were performed to identify the structure of the CT complex in the aqueous solution upon the addition of TCNQ. The cryo-TEM image of **1** complexed with 0.5 equivalents of TCNQ revealed isolated 2D objects with lateral dimensions of several micrometers, demonstrating that the sheets are robust and free-standing in the bulk solution (Figure 2D). The negatively stained TEM image obtained using a cast film indicated flat 2D sheet structures, consistent with the cryo-TEM result (Figure 3A). Atomic force microscopy (AFM) experiments revealed that the sheets were flat and uniform, with a thickness of 4.5 nm (Figure 2E). X-ray diffraction performed on the films prepared via the freeze-drying of the aqueous solution provided a reflection of 4.4 nm as the *d*-spacing between sheets, consistent with the thickness obtained from the AFM results (Figures 2F, S8, and S9).

When the CT complexes were subjected to CD measurements, apparent CD signals were detected, with a strong Cotton effect in the spectral range of the aromatic segments, in contrast with the solution before TCNQ addition (Figures 2C and S10). These results indicated that the resulting supramolecular sheets, driven by TCNQ, are chiral by asymmetric stacking of the aromatic segments, attributed to the transfer of the molecular chirality of the D-mannose to the chirality of the co-assembled structures (Figure 2G). We performed density functional theory (DFT) calculations to further understand the supramolecular chirality induction. The M06-2X (6-31G*) basis set in which mid-range interactions are important was used to demonstrate the aromatic stacked systems.[19] The calculation results showed a faced-centered stacking of two methoxypyrene and one TCNQ in the complex. Furthermore, the chirality could be explained by an asymmetry of two methoxy groups in the pyrene in the same direction (Figure 2G). Time-dependent DFT (TD-DFT) calculations of the CT complex were performed to predict electronic CD spectra of

E1 and E2 for understanding the chiral direction. As a result, the simulation of the E1 type agrees well with the experimental observations (Figure 2G).

2.2 | Spontaneous disassembly of supramolecular chiral sheets

Notably, as a function of time, after the addition of TCNQ, CD signals and CT absorption bands disappeared gradually, accompanied by a color change of the solution from yellow to blue. Eventually, the spectroscopic results reverted to those observed before adding TCNQ (Figure 3B, C). The sample solutions after aging were subjected to high-performance liquid chromatography (HPLC) analysis to investigate the disappearance of spectral signals corresponding to donor–acceptor interactions. As shown in Figure S11, no TCNQ could be detected, whereas amphiphile **1** remained intact over time. Indeed, a new broad absorption peak corresponding to the TCNQ anion, which could disrupt donor-acceptor interactions, was detected at approximately 630 nm (Figures 3C and S12).[20] As photo-induced TCNQ reduction in an aqueous solution has been reported,[21,22] chiral sheet solutions were separately kept under ambient light and in a darkroom and investigated by analyzing their absorption and CD spectra to understand the formation of the TCNQ anion. The absorbance at 441 nm and the CD intensity at 465 nm for the sheet solution in the darkroom did not decrease during 7 days of aging, which indicates that the photoreduction of TCNQ to the anion occurred under ambient light conditions (Figure S13). In the photoreduction of TCNQ, the cation of the solvent molecule is reported to be the counter partner of the TCNQ anion generating an oxygen molecule in the aqueous solution (Figure 1).[21,22] Negatively stained TEM images revealed that the TCNQ-driven supramolecular chiral sheet structures were disassembled from the sheet edges over time and eventually disappeared entirely within seven days, triggered by the dissipated solution, CD signals and the CT absorption band could not be induced (Figure 3A). Although an oxidant was added to the TCNQ anion in the dissipated solution, CD signals and the CT absorption band could not be induced (Figure S18).[23] The results indicated that the reduction of TCNQ to the anion was irreversible. Therefore, pristine TCNQ was subsequently added to amphiphile **1**. Notably, the subsequent addition of TCNQ induced the formation of chiral sheets repeatedly without sacrificing the donor–acceptor interaction characterized by CD spectroscopy, thereby enabling the assembly and disassembly cycles of supramolecular chiral sheets (Figures 1B, 3C, and S14). Considering all the data, we have demonstrated the generation of switchable supramolecular chiral sheets driven by spontaneous TCNQ reduction.

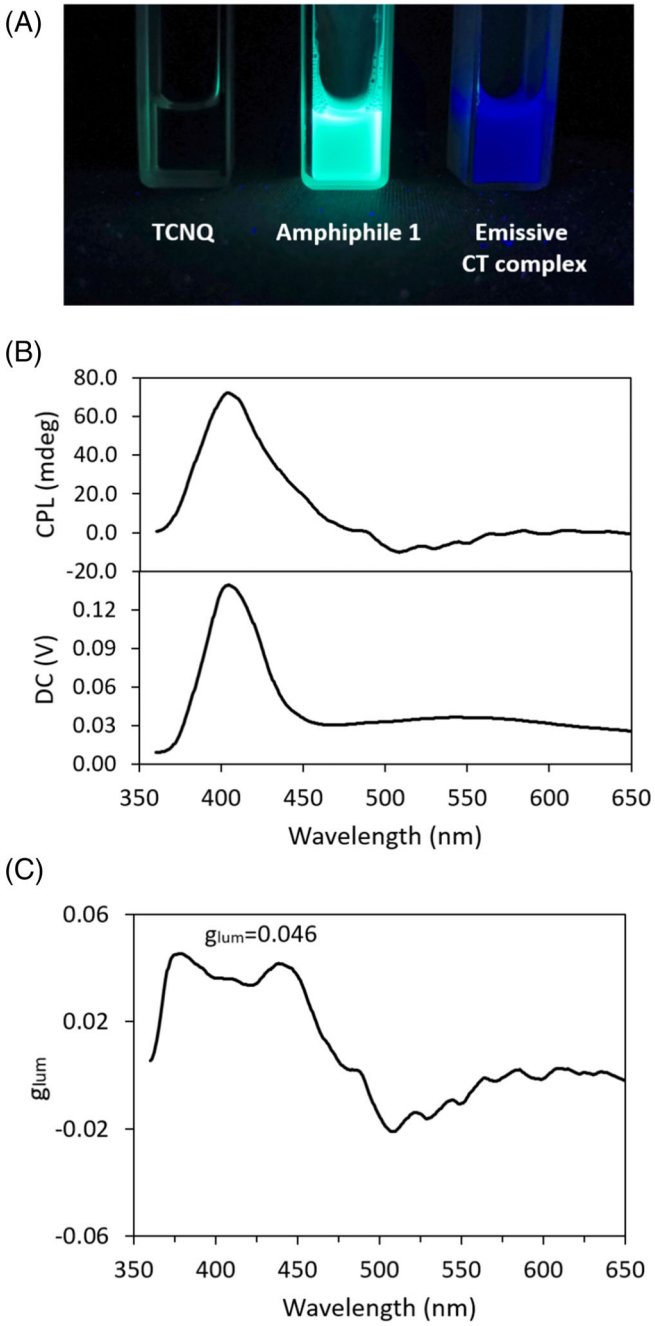

FIGURE 4 Supramolecular chiral sheets showing CPL. (A) Optical image of TCNQ (in CH_3CN), **1** (in H_2O), and CT complex (in H_2O) solution with the concentration of 314 μM under 365 nm UV light. (B) CPL spectrum and (C) g_{lum} plot of **1** (314 μM) with 0.5 equivalents of TCNQ in an aqueous solution. Excitation wavelength = 343 nm.

2.3 | Chiral sheets showing CPL

Because the TCNQ-driven supramolecular sheets were accompanied by significant CD signals and fluorescent emission, CPL experiments were performed to investigate the chiroptical properties of the chiral sheets containing

the emissive CT complex. Generally, the CT complexes have a relatively large magnetic dipole transition moment and a forbidden electron dipole transition moment, which are important factors contributing to a high g_{lum} in CPL. Hence, a high g_{lum} would imply that the resulting emissive CT complex sheet can be expected to be a CPL-active material.[17] Indeed, an intense positive CPL peak was detected in the solution state under an excitation wavelength of 343 nm. The g_{lum} value for the sheets was calculated as 0.046, which is significantly higher than recently reported g_{lum} values for chiral CT complexes (Figure 4).[17] The CPL emission likewise disappeared upon the dissipation of TCNQ, implying the presence of switchable chiroptical supramolecular materials driven by TCNQ photoreduction. Considering the varied applications of CPL materials, such as in bionanomaterials, CPL displays, sensing, and probing,[24] switchable CPL materials can provide new strategies for the development of dynamic CPL materials.

3 | CONCLUSION

We have obtained supramolecular chiral 2D materials via donor–acceptor interactions between pyrene-based amphiphile **1** and TCNQ. The chiral sheets containing an emissive CT complex, where the aromatic segments such as pyrene and TCNQ adopt asymmetric stacking, exhibited intense CPL with a considerable g_{lum} value. Remarkably, the donor-acceptor interaction disappeared over time due to the irreversible photoreduction of TCNQ into a TCNQ anion, enabling the spontaneous disassembly of the supramolecular sheets to amphiphile **1**. Subsequent additions of TCNQ could activate the chiral sheets repeatedly, demonstrating the existence of switchable supramolecular chiral sheets driven by TCNQ through donor-acceptor interactions. Such a unique chiral 2D material may provide new insights into functional systems for artificial membranes with chiral optics.

4 | EXPERIMENTAL SECTION/ METHODS

4.1 | General methods

All reactions were performed in oven-dried glassware under a dry argon atmosphere. Tetrahydrofuran (THF) was dried by distillation from sodium-benzophenone immediately before use. Dichloromethane (DCM) was dried by distillation from CaH_2. Distilled water was polished by ion exchange and filtration. Other solvents and organic reagents were purchased from commercial vendors and used without further purification unless otherwise mentioned. The reactions were monitored by thin-layer chromatography (TLC; Merck, silica gel 60 F_{254} 0.25 mm) with visualization under UV light (254 and 365 nm) or treating iodine and phosphomolybdic acid. The products were purified by flash column chromatography on silica gel (230–400 meshes). Preparative HPLC was performed for further purification of the final desired molecules by using Prominence LC-20AP (SHIMADZU) and YMC C8 reverse phase column (250 × 4.6 mm I.D., S-5 μm, 12 nm and 250 × 20.0 mm I.D., S-5 μm, 12 nm). ^{1}H-NMR and ^{13}C-NMR spectra were recorded on Bruker AVANCE III 500. All compounds were subjected to ^{1}H NMR analysis to confirm ≥98% sample purity. Multiplicity was indicated as follows: s (singlet), d (doublet), t (triplet), q (quartet), quin (quintet), m (multiplet), dd (doublet of doublets), dt (doublet of triplets), td (triplet of doublets), br s (broad singlet). Coupling constants are reported in Hertz (Hz). Matrix-assisted laser desorption/ionization time of flight mass spectrometry (MALDI-TOF-MS) was performed on a Bruker Microflex LRF20 using α-cyano-4-hydroxycinnamic acid (CHCA) as a matrix. UV/Vis spectra were obtained from a Hitachi U-2900 Spectrophotometer. Fluorescence spectra were obtained from a Hitachi F7000 Fluorescence Spectrophotometer. CD spectra were obtained from a JASCO J-810 spectropolarimeter. CPL spectra were obtained from a JASCO CPL-200. X-ray scattering measurements were performed in transmission mode with synchrotron radiation at the 3C X-ray beamline at the Pohang Accelerator Laboratory, Korea.

4.2 | TEM experiments

To investigate the self-assembled structures in aqueous solution, a drop of each sample solution was placed on a carbon-coated copper grid (Carbon Type B (15–25 nm)) on 200 meshes, with (Formvar; Ted Pella, Inc.), and the solution was allowed to evaporate under ambient conditions. These samples were stained by depositing a drop of uranyl acetate aqueous solution (0.4–1.0 wt%) on the surface of the sample-loaded grid. The dried specimen was observed by a JEOL-JEM HR2100 operated at 120 kV. The cryo-TEM experiments were performed with a thin film of an aqueous solution of amphiphiles (3 μl) transferred to a lacey-supported grid. The thin aqueous films were prepared under controlled temperature and humidity conditions (97%–99%) within a custom-built environmental chamber to prevent water evaporation from the sample solution. The excess liquid was blotted with filter paper for 2–3 s. The thin aqueous films were rapidly vitrified by plunging them into liquid ethane (cooled by liquid nitrogen) at their freezing point. The grid was transferred, on a

Gatan 626 cryo holder, using a cryo-transfer device and transferred to the JEOL-JEM HR2100 TEM. Direct imaging was carried out at a temperature of approximately −175°C and with a 120 kV accelerating voltage, using the images acquired with a Dual vision 300 W and SC 1000 CCD camera (Gatan, Inc.; Warrendale, PA). The data were analyzed using the Digital Micrograph software.

4.3 | AFM experiments

The sample films on the mica surface were prepared by evaporation of sample solutions. The measurements were conducted on a MultiMode 8 AFM with NanoScope V controller, NanoScope software, and NanoScope Analysis software (Bruker AXS Corporation, Santa Barbara, CA, USA) in the air at an ambient temperature (ca. 25 °C) in the tapping mode.

4.4 | Sampling methods

Amphiphile **1** in MeOH and TCNQ in CH_3CN were mixed, and the solvents were evaporated under reduced pressure. Deionized water was added to the dried mixture to 314 μM concentration, and then the aqueous solution was sonicated for 30 min in a cold bath.

4.5 | Molecular simulations

Analysis of the packing mode amphiphile **1** and TCNQ co-assembled sheet structure was optimized using the DFT M06-2X (6-31G*) method using Gaussian 09 software. CD spectra of the complex were simulated by time-dependent density functional theory via the M06-2X method with a 6-31G*+ basis-set.

ACKNOWLEDGMENTS

We applied the SDC approach for the sequence of authors. This work was supported by the National Natural Science Foundation of China (No. 21971084, 92156023, and 22150710515), the National Research Foundation of Korea (NRF) grant funded by the Korea government (MSIT) (NRF-2022R1F1A1075138, and NRF-2022R1A4A1031687), a Korea University grant, and KU-KIST School Fund.

ORCID

Yongju Kim https://orcid.org/0000-0002-5862-5228
Myongsoo Lee https://orcid.org/0000-0002-5315-3807

REFERENCES

[1] E. Mattia, S. Otto, *Nat. Nanotechnol.* **2015**, *10*, 111.
[2] X. Ma, Y. Zhao, *Chem. Rev.* **2015**, *115*, 7794.
[3] E. Busseron, Y. Ruff, E. Moulin, N. Giuseppone, *Nanoscale* **2013**, *5*, 7098.
[4] S. I. Stupp, L. C. Palmer, *Chem. Mater.* **2014**, *26*, 507.
[5] A. V. Davis, R. M. Yeh, K. N. Raymond, *Proc. Natl. Acad. Sci. USA.* **2002**, *99*, 4793.
[6] M. Liu, L. Zhang, T. Wang, *Chem. Rev.* **2015**, *115*, 7304.
[7] M. A. Mateos-Timoneda, M. Crego-Calama, D. N. Reinhoudt, *Chem. Soc. Rev.* **2004**, *33*, 363.
[8] P. Xing, Y. Zhao, *Acc. Chem. Res.* **2018**, *51*, 2324.
[9] T. D. Crawford, M. C. Tam, M. L. Abrams, *J. Phys. Chem. A.* **2007**, *111*, 12057.
[10] M. Saba, M. Thiel, M. D. Turner, S. T. Hyde, M. Gu, K. Grosse-Brauckmann, D. N. Neshev, K. Mecke, G. E. Schröder-Turk, *Phys. Rev. Lett.* **2011**, *106*, 103902.
[11] R. Carr, N. H. Evans, D. Parker, *Chem. Soc. Rev.* **2012**, *41*, 7673.
[12] A. Adam, G. Haberhauer, *J. Am. Chem. Soc.* **2017**, *139*, 9708.
[13] W. Miao, S. Wang, M. Liu, *Adv. Funct. Mater.* **2017**, *27*, 1701368.
[14] B. Shen, Y. Kim, M. Lee, *Adv. Mater.* **2020**, *32*, 1905669.
[15] Y. Luo, C. Chi, M. Jiang, R. Li, S. Zu, Y. Li, Z. Fang, *Adv. Opt. Mater.* **2017**, *5*, 1700040.
[16] H. Sun, M. Wang, X. Wei, R. Zhang, S. Wang, A. Khan, R. Usman, Q. Feng, M. Du, F. Yu, W. Zhang, C. Xu, *Cryst. Growth des.* **2015**, *15*, 4032.
[17] J. Han, D. Yang, X. Jin, Y. Jiang, M. Liu, P. Duan, *Angew. Chem. Int. Ed.* **2019**, *58*, 7013.
[18] W. T. M. V. Gompel, R. Herckens, K. V. Hecke, B. Ruttens, J. D'Haen, L. Lutsen, D. Vanderzande, *Chem. Commun.* **2019**, *55*, 2481.
[19] S. Green, M. A. Fox, *J. Phys. Chem.* **1995**, *99*, 14752.
[20] H. Shiozawa, B. C. Bayer, H. Peterlik, J. C. Meyer, W. Lang, T. Pichler, *Sci. Rep.* **2017**, *7*, 2439.
[21] L. Ma, P. Hu, C. Kloc, H. Sun, M. E. Michel-Beyerle, G. G. Gurzadyan, *Chem. Phys. Lett.* **2014**, *609*, 11.
[22] C. Zhao, M. A. Bond, *J. Am. Chem. Soc.* **2009**, *131*, 4279.
[23] M. C. Grossel, A. J. Duke, D. B. Hibbert, I. K. Lewis, E. A. Seddon, P. N. Horton, S. C. Weston, *Chem. Mater.* **2000**, *12*, 2319.
[24] Y. Sang, J. Han, T. Zhao, P. Duan, M. Liu, *Adv. Mater.* **2020**, *32*, 1900110.

SUPPORTING INFORMATION

Additional supporting information can be found online in the Supporting Information section at the end of this article.

How to cite this article: L. Dong, D. Lee, Y. Kim, M. Lee, *J. Polym. Sci.* **2023**, *61*(10), 979. https://doi.org/10.1002/pol.20220745